NeuroImage: Clinical 35 (2022) 103100

Contents lists available at ScienceDirect

NeuroImage: Clinical

journal homepage: www.elsevier.com/locate/ynicl

Neural correlates of working memory and compensation at different stages of cognitive impairment in Parkinson's disease

Takaaki Hattori [a,b,*], Richard Reynolds [c], Edythe Wiggs [b], Silvina G. Horovitz [b], Codrin Lungu [d], Gang Chen [c], Eiji Yasuda [a], Mark Hallett [b]

[a] Tokyo Medical and Dental University, Department of Neurology and Neurological Science, Japan
[b] Human Motor Control Section, National Institute of Neurological Disorders and Stroke, National Institutes of Health, United States
[c] Scientific and Statistical Computing Core, National Institute of Mental Health, United States
[d] Division of Clinical Research, National Institute of Neurological Disorders and Stroke, National Institutes of Health, United States

ARTICLE INFO

Keywords:
Parkinson's disease
Working memory
fMRI
Compensation

ABSTRACT

Working memory (WM) impairment is one of the most frequent cognitive deficits in Parkinson's disease (PD). However, it is not known how neural activity is altered and compensatory responses eventually fail during progression. We aimed to elucidate neural correlates of WM and compensatory mechanisms in PD. Eighteen cognitively normal PD patients (PD-CogNL), 16 with PD with mild cognitive impairment (PD-MCI), 11 with PD with dementia (PDD), and 17 healthy controls (HCs) were evaluated. Subjects performed an n-back task. Functional MRI data were analyzed by event-related analysis for correct responses. Brain activations were evaluated by comparing them to fixation cross or 0-back task, and correlated with n-back task performance. When compared to fixation cross, PD-CogNL patients had more activation in WM areas than HCs for both the 2- and 3-back tasks. PD-MCI and PDD patients had more activation in WM areas than HCs for the 0- and 1-back task. 2-back task performance was correlated with brain activations (vs. 0-back task) in the bilateral dorsolateral prefrontal cortex and frontal eye field (FEF) and left rostral prefrontal cortex, caudate nucleus, inferior/superior parietal lobule (IPL/SPL), and anterior insular cortex as well as anterior cingulate cortex. 3-back task performance was correlated with brain activations (vs. 0-back task) in the left FEF, right caudate nucleus, and bilateral IPL/SPL. Additional activations on top of the 0-back task, rather than fixation cross, are the neural correlates of WM. Our results suggest PD patients have two types of compensatory mechanisms: (1) Hyperactivation for different WM load tasks depending on their cognitive status. PD-CogNL have hyperactivation for moderate and heavy working memory load tasks while maintaining normal working memory performance. In contrast, PD-MCI and PDD have hyperactivation for control task and light working memory load task, leaving less neural resources to further activate for more demanding tasks and resulting in impaired working memory performance. (2) Bilateral recruitment of WM-related areas, in particular the DLPFC, FEF, IPL/SPL and caudate nucleus, to improve WM performance.

1. Introduction

Cognitive impairment is a common non-motor symptom in Parkinson's disease (PD) patients, and it can severely hamper the daily lives of patients as well as their caregivers. Cognitively normal PD (PD-CogNL) patients often develop PD with mild cognitive impairment (PD-MCI) and eventually progress to PD with dementia (PDD). PD-MCI is seen in around 10 to 35 percent of early PD patients (Muslimovic et al., 2005, Weintraub et al., 2015). PDD was found in approximately 30 percent of PD patients in a cross-sectional study (Aarsland et al., 2005, Svenningsson et al., 2012). While many types of cognitive functions can be impaired in PD patients, working memory (WM) is one of the most frequently affected cognitive domains in these patients (Lewis et al., 2003, Lewis et al., 2005, Beato et al., 2008, Goldman et al., 2014). WM is an essential cognitive ability that is also used within other cognitive processes to temporarily hold and manipulate information (Baddeley

* Corresponding author at: Department of Neurology and Neurological Science, Graduate School of Medical and Dental Sciences, Tokyo Medical and Dental University, 1-5-45, Yushima, Bunkyo-ku, Tokyo 113-8519, Japan.
E-mail address: takaaki-hattori@umin.ac.jp (T. Hattori).

https://doi.org/10.1016/j.nicl.2022.103100
Received 5 February 2022; Received in revised form 9 May 2022; Accepted 23 June 2022
Available online 27 June 2022

2010). It is known that multiple brain areas are involved in WM processing, and each brain area is engaged in a specialized function such as strategic control of WM, parallel processing, attentional control, and WM storage (Owen et al., 2005).

Dopaminergic denervation plays a pivotal role in the pathogenesis of PD (Antonelli and Strafella, 2014, Poewe et al., 2017). Dopaminergic neurons in the substantia nigra project to the striatum via the nigrostriatal pathway and the prefrontal cortex via the mesocortical pathway (Klein et al., 2019). The dorsolateral prefrontal cortex (DLPFC) and the rostral prefrontal cortex (RPFC) are parts of WM-related areas that are directly affected from the impaired dopaminergic mesocortical pathway originating from the ventral tegmentum area (Alexander et al., 1986, Oades and Halliday, 1987). DLPFC and RPFC are also indirectly influenced by the impaired dopaminergic nigrostriatal pathway via the striatothalamocortical loops (Alexander et al., 1986). Dopaminergic denervation underlies WM impairment and executive dysfunction in PD patients (Dirnberger and Jahanshahi, 2013, Gratwicke et al., 2015). In fact, dopaminergic replacement improves spatial WM, whereas nonspatial WM is unaltered (Macdonald and Monchi, 2011, Baggio and Junqué, 2019).

In functional magnetic resonance imaging (fMRI) analysis, neural activity is represented by the blood oxygenation level-dependent (BOLD) effect estimate (Ogawa et al., 1990). A BOLD effect estimate is typically calculated by fitting the data to an idealized hemodynamic response curve using a linear regression model. The latter quantifies the extent of activation while performing the task compared to performing a control task or starting at fixation cross. Here, we used the n-back task to evaluate WM in PD patients (Kirchner 1958). The 0-back task is the control task in which subjects respond to either a prespecified or a different letter by pressing a button. The 1, 2 and 3-back task requires subjects to respond whether the current letter is the same as the letter presented n trials before or not. Both tasks require motor response, attention, and decision making, but the 0-back task does not require a typical "WM". Thus, comparing 1, 2 or 3-back vs. 0-back reflects "WM" proper. In contrast, staring at a fixation cross is more like a task-free state that does not require a subject to respond. Comparing 0, 1, 2 or 3-back to a fixation cross reflects all task components including those present in 0-back. The BOLD effect estimates are different when compared to either 0-back task or fixation cross (Fig. 1A). Therefore, we evaluated two BOLD effect estimates to better understand the neural correlates of WM and neural activity in PD patients.

This study used a novel fMRI denoising method, called multi-echo independent component analysis (ME-ICA) (Kundu et al., 2017). While the BOLD signal has echo-time dependence, noise such as motion, physiological artifacts, and signal drifts due to heating of MRI over the scanning does not have echo-time dependence. ME-ICA takes advantage of this phenomenon and classifies ICA-components as either BOLD signal or noise. ME-ICA is a robust denoising method in a data-driven way, successfully improving signal to noise ratio (Kundu et al., 2017). It has been shown that ME-ICA is effective for denoising not only resting-state fMRI data, but also task-based fMRI data (Gonzalez-Castillo et al., 2016).

Several previous studies investigated brain activation patterns during WM tasks in PD patients. PD-CogNL patients have compensatory hyperactivation in the bilateral putamen when OFF medication; dopaminergic medication normalizes the hyperactivation (Poston et al., 2016). Trujillo et al. (2015) reported that de novo PD patients have hyperactivation in the bilateral DLPFC, left caudate nucleus (CdN), and the left inferior parietal lobule (IPL) while performing a visuospatial WM task. On the other hand, PD patients with executive dysfunction or MCI have reduced activation in CdN (Lewis et al., 2003a,b) or the right dorsal CdN and the bilateral anterior cingulate cortex (ACC) (Ekman et al., 2012) during a WM task, respectively, compared with PD-CogNL patients. However, a recent meta-analysis showed that the current literature is not entirely consistent regarding neural correlates of executive or WM impairment in PD (Giehl et al., 2019). Moreover, no studies explored how brain activation patterns are altered and compensatory mechanisms work and fail in PD patients, especially including PDD patients that are underrepresented in the current literature.

Based on the previous studies, we hypothesized that PD patients have malfunction in WM-related areas, especially left DLPFC, and in deactivated areas such as the default mode network (DMN) (Shulman et al., 1997, Raichle et al., 2001, Raichle 2015), especially the posterior cingulate cortex (PCC), depending on cognitive status. We included all those areas in region of interest (ROI) analysis. On the other hand, this is the first study using ME-ICA for n-back task in PD patients, especially including PDD patients. Therefore, we used exploratory design to quantify all ROIs, rather than specifying limited ROIs.

Here, we aimed to elucidate neural correlates and compensatory mechanisms for WM impairment among PD patients with different levels of cognitive function using ME-ICA analysis for fMRI data during an n-back task.

2. Methods

2.1. Participants

PD patients were recruited from the Human Motor Control clinic at the National Institutes of Health (NIH) between April 2013 and May

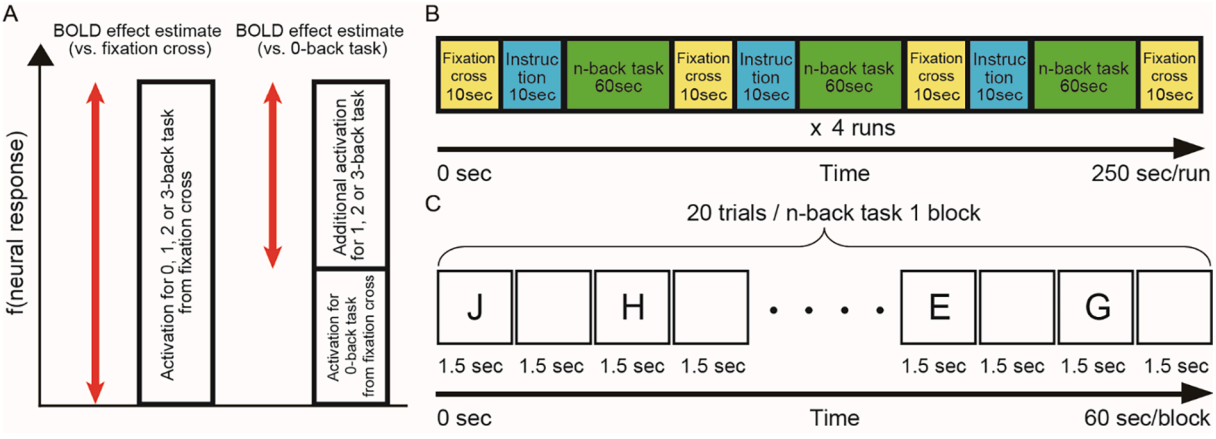

Fig. 1. Two BOLD effect estimates and structure of n-back task. (A) BOLD effect estimate (vs. fixation cross) is equivalent to activation during n-back task from fixation cross. BOLD effect estimate (vs. 0-back task) is equivalent to additional activation during 1, 2 or 3-back task on top of 0-back task. (B) Structure of 1 run is presented. All subjects performed 4 runs in pseudo-randomized order. (C) Structure of n-back task for 1 block is presented. A sequence of letters is presented on the screen every 3 s and shown for 1.5 s followed by 1.5 s of a blank screen. A total of 20 trials is performed in 1 block. BOLD = blood oxygenation level-dependent.

2014. Age- and sex-matched healthy controls (HCs) were recruited from the NIH Clinical Research Volunteer Program database. PD was diagnosed by movement disorders neurologists, C.L. and M.H., in the NIH Parkinson Clinic according to the clinical diagnostic criteria of the Parkinson's Disease United Kingdom Brain Bank (Hughes et al., 1992). All subjects were right-handed and their first language was English. Subjects abstained from caffeine and alcohol for 24 h before each visit. All subjects were tested by the Beck Depression Inventory-II (BDI-II). Subjects who met the following conditions were excluded: reported use of illegal drugs within the past 6 months, >7 alcoholic drinks a week for females or 14 alcoholic drinks a week for males, BDI-II > 29 (cut-off to define severe depression (Wang and Gorenstein, 2013)) or history of a neurologic disorder such as a brain tumor, stroke and head injury with loss of consciousness. All PD patients took daily doses of anti-Parkinsonian medications as scheduled. Parkinsonism was evaluated by using the Movement Disorder Society-Sponsored Revision of the Unified Parkinson's Disease Rating Scale (MDS-UPDRS) (Goetz et al., 2008). Levodopa equivalent dose (LED) was calculated according to a previous study (Tomlinson et al., 2010). All subjects were evaluated by comprehensive cognitive assessment described below. All patients had a clinical interview by a neurologist to identify whether the patient fulfilled the core features of PDD according to published diagnostic criteria (Emre et al., 2007): (1) there was a decline from premorbid level, and (2) deficits were severe enough to impair daily life (social, occupational, or personal care). In order to make a dignosis of PDD, we followed published diagnostic procedures for PDD (Dubois et al., 2007) by considering the patient's medical record, the interview with patient, and all assessments. Patients not meeting criteria for PDD, were classified as either PD-CogNL or PD-MCI. PD-MCI was diagnosed according to published diagnostic criteria (Litvan et al., 2012). This requires at least 2 abnormal tests showing Z-score of > 2 or < -2. These deficits can be in the same or different cognitive domains. Patients not meeting either criteria were classified as PD-CogNL.

This study was approved by Institutional Review Board of National Institute of Neurological Disorders and Stroke (NINDS), NIH. All the participants who had consent capacity gave their written informed consent to the study. For patients who did not have consent capacity, the designated durable power of attorney delegate gave written informed consent.

2.2. Neuropsychological assessments

Global cognition was evaluated by the Mini-Mental State Examination (MMSE) and Montreal Cognitive Assessment test (MoCA). Frontal lobe function was evaluated by the Frontal Assessment Battery (FAB).

Comprehensive cognitive assessment was performed for all subjects by neuropsychologists (E.W. and M.T.). Five cognitive domains were evaluated using at least two sets of batteries for each cognitive domain as follows: (1) Executive function: Wisconsin card sorting test and the Trails, Verbal Fluency, Sorting, and Tower subtests of Delis-Kaplan Executive Function System; (2) Visuospatial function: the Visual Object and Space Perception Battery; (3) Language: the Boston Naming Test and sum of language subscores of the MMSE (maximum 8 points); (4) Memory: total scores for trials 1–5 of The California Verbal Learning Test - II and sum of registration and recall subscores of the MMSE (maximum 6 points); and (5) Attention and Working Memory: digit span and letter number sequencing subtests in the Wechsler Adult Intelligence Scale - III. Each score was converted to a z-score by using age-matched norms or scores of HCs in this study when there were no available norms. An abnormal score of the test was defined by a z-score which was>2 or smaller than −2.

2.3. MRI data acquisition

All subjects were scanned in a 3 Tesla MRI scanner (SIEMENS, Skyra) using a 32-channel head coil. Subjects lay in the scanner in supine position with their head fixed using foam pads. A series of scans, including arterial spin labelling, resting-state fMRI, task fMRI while performing the n-back task, structural MRI, and diffusion tensor imaging were obtained during 80 min of scanning. Here, we used task fMRI data while performing n-back task and structural MRI for analysis. For task fMRI we used a T2-weighted multi-echo planar imaging sequence (TE = 11, 22.4, 33.9 ms, TR = 2000 ms, flip angle = 70, FOV = 210 × 210 mm, voxel size = 3 × 3 × 3 mm, acceleration factor 3, number of slices = 34, interleaved, bandwidth 2552 Hz/Px). For structural data, three-dimensional-T1 weighted (3D-T1) MRI images were obtained by using multi-echo time magnetization prepared rapid acquisition gradient echo (MEMPRAGE) sequence (TE = 1.69, 3.55, 5.41, 7.27 ms, TR = 2530 ms, TI = 1,100 ms, flip angle = 7, FOV = 256 × 256 mm, voxel size = 1 × 1 × 1 mm, 1 mm sagittal slices, acceleration factor 2, number of slices = 176, acquisition time = 6 min 2 s).

2.4. n-back task

Before entering the MRI scanning room, subjects were shown how to perform the n-back task by the same investigator, T.H. After instructions, subjects were asked to verbally explain how to perform the n-back task. When the subjects could explain correctly, they were asked to perform a practice test on paper. If a subject's explanation was wrong or a subject gave the wrong response from lack of understanding, the same instruction was repeated until the subject could perform without misunderstanding. Stimuli were generated using E-Prime software (v2.0; Psychology Software Tools, Pittsburgh, PA; 2002) and presented at the center of the screen with a magnet-compatible projection system. Subjects viewed the screen via a mirror positioned in front of their eyes. Subjects performed 4 runs of the n-back task, lasting 250 s each. Each run included 3 blocks, consisting of 10 s fixation cross, 10 s instruction, and 60 s of n-back task (Fig. 1B). Runs started with 10 s fixation cross that were discarded for T1 equilibration. Runs ended with 10 s fixation cross. During the instruction period, the next n-back task was displayed on screen. In total, three blocks of each n-bask task were presented, in a pseudo-randomized order, avoiding repetition of the same tasks within a run. Total scanning time for task fMRI was 16 min and 40 s. During n-back blocks, a sequence of letters was presented on the screen every 3 s and shown for 1.5 s followed by 1.5 s of a blank screen (Fig. 1C). Subjects were required to respond each time by pressing a right or left button to indicate whether the current letter was the same as the previous n-back letter or not. In the 0-back task, the target letter 'X' was the correct letter and other letters were wrong letters. In other n-back tasks (n = 1, 2 and 3), when a presented letter was the same as the letter presented n trials back, the letter was correct. Responses were recorded for each trial. Accuracy for the n-back task was evaluated with the d-prime index (Haatveit et al., 2010). d-prime index is calculated from the formula d-prime index = $Z_{hit} - Z_{false\ alarm}$. Z represents a transformation of hit rate or false-alarm rate. Thus, d-prime index quantifies the normalized distance between signal and noise and noise alone (Haatveit et al., 2010).

2.5. MRI data processing

MRI data processing was carried out using the **A**nalysis of **F**unctional **N**euro**I**mages (AFNI) (Cox 1996). The MEMPRAGE images were averaged across 4 echoes and used for registration. The first 5 volumes of each run of fMRI data were discarded to allow for T1 equilibration. ME-ICA was performed to denoise fMRI data using the AFNI program: meica.py, as previously described (Kundu et al., 2012). In summary, 4 runs of fMRI data were independently preprocessed by performing slice timing correction, spatially normalization to the MNI_caez_N27 template. The preprocessed 4 runs were concatenated, and TE-dependence analysis was performed by using the AFNI program: tedana.py. Then denoised time course data were generated by removing non-BOLD signals. The event-related fMRI analysis was performed for the denoised fMRI data using the AFNI program afni_proc.py. The fMRI data were smoothed

with a 6.0-mm full-width-half-maximum Gaussian kernel and analyzed with regressors for the sustained activity during instruction using a command option "GAM (8.6, 0.547, 10)" and the transient activity such as hit, miss, false alarm, correct rejection, and no responses during performing n-back task using a command option "GAM (8.6, 0.547)". Only the correct responses (hits and correct rejections) were included in the group level analysis which generated 2 contrasts: (1) between 0-, 1-, 2- or 3-back task and fixation cross and (2) between 1-, 2- or 3-back task and 0-back task (Fig. 1A).

2.6. Regions of interest analysis

To understand the neural correlates of working memory and compensation at different stages of cognitive impairment in PD, we defined the WM areas using the full dataset, irrespective of group or cognitive status. ROIs were created by comparing n = 1-, 2- and 3-back tasks with the 0-back task in all subjects. This allowed for including the traditional WM areas, but also areas that might be related to the deficits.

In order to create ROI masks for WM-related areas, the cut-off criterion was set at the corrected p value < 0.05 defined by 3dClustim ($p < 2 \times 10^{-4}$ and voxel > 20). A smaller p-value was used to create separate ROI masks for the areas whose borders overlap.

2.7. Voxel-based correlation analysis with d-prime index

To identify the anatomical regions whose extent of activation is associated with performance of the n-back task in PD patients, voxel-based correlation analysis was performed for two BOLD effect estimates (vs. fixation cross or vs. 0-back task) and the d-prime index in all PD patients by using AFNI program: 3dttest++. The voxel-based correlation analysis was performed only within the cerebrum because the field of view of fMRI did not cover either the entire brainstem or the cerebellum.

2.8. Study size

A previous study showed that WM performance and brain activation were correlated with a correlation coefficient of 0.47 in cognitively unimpaired PD patients (Poston et al., 2016). To obtain 80% power to test the null hypothesis of no correlation compared to a correlation coefficient of 0.48, with a significance level of 0.05, a total of 33 PD patients was required.

2.9. Statistical analysis

The assumption of normality was evaluated based on the residuals using the Shapiro-Wilk test. The equality of variances was evaluated by Levene's test. Statistical analysis of demographic and clinical data was performed using the Scientific Package for Social Sciences version 11 (SPSS, Chicago, IL): analysis of variance with post-hoc Turkey's HSD test for parametric test, Kruskal-Wallis test with post-hoc Mann-Whitney U-tests for non-parametric test, or χ^2 test for categorical data. The criterion of statistical significance was $p < 0.05$.

BOLD effect estimates (vs. fixation cross or vs. 0-back task) in ROIs were compared among 3 patient groups and HC group using a Bayesian multilevel model that incorporated all the ROIs into a hierarchical framework using the program "RBA" in AFNI (Chen et al., 2019). In addition, inter-task difference were also assessed by comparing BOLD effect estimates (vs. fixation cross) in ROIs among different loads of n-back tasks. Specifically, with y_{ij} as the BOLD effect of the ith ROI from the jth subject, we formulated the Bayesian multilevel model with a Gaussian likelihood,

$$y_{ij} \sim N\left(b + \theta_i + \tau_j, \sigma^2\right), i = 1, 2, \cdots, k, j = 1, 2, \cdots, n,$$

where b is the overall intercept, θ_i represents the effect at the ith ROI while τ_j codes the effect from the jth subject, and σ^2 is the distributional variance. Two prior distributions were adopted for the cross-subject and cross-region variability: $\theta_i \sim N\left(0, \lambda^2\right)$ and $\tau_j \sim N\left(0, \pi^2\right)$. The population-level inferences for each of the k ROIs were assessed per the overall posterior distribution from Markov chain Monte Carlo simulations. In contrast to the conventional modeling methodology of massively univariate analysis in which each region is handled separately, the Bayesian approach incorporates the data hierarchy with information efficiently shared and regularized across regions in a single model; therefore, no multiple testing adjustment is needed, avoiding excessive penalty (Chen et al., 2021). For inter-group comparisons, we labelled the results with * that indicate strong evidence for inter-group difference based on the posterior probability of a positive or negative effect being<0.05. However, we emphasize such a criterion should not be rigorously taken as a dichotomization process for two reasons. First, the statistical evidence is a continuous spectrum, and any cutoff value is arbitrary and artificial. Second, all results and evidence should be considered and shown regardless of their strength to avoid potential biases (Chen et al., 2020). For simplicity, all results were shown only for inter-task comparisons.

For voxel-based correlation analysis, the significance criterion was set at corrected p value < 0.05 defined by 3dClustim ($p < 0.003$, t-value $= 3.14$, correlation coefficient r = 0.43, and voxel > 82).

3. Results

We excluded 9 PD patients because of a data processing error (n = 2), presence of abnormal brain lesions (n = 3), and the inability to perform n-back task (n = 4). We also excluded 3 HCs because of a data processing error (n = 1) and the presence of abnormal brain lesions (n = 2). Demographic and clinical data of enrolled patients in PD subgroups or HCs are summarized in Table 1. There was no significant inter-group difference for age, sex, disease duration, and length of education. MDS-UPDRS part II, III, and Hoehn-Yahr stage were significantly higher in PDD than in PD-MCI. As quality control, we confirmed that the number of BOLD components derived from ME-ICA preprocessing did not differ among the 4 groups (Table 1). Results of neuropsychological assessments are described in Table 2. BDI-II score was higher in all PD subgroups than HCs. There are many inter-group differences in accuracy rate and d-prime index in n-back task and neuropsychological assessments, as shown in Tables 1 and 2 and Fig. 7C. In summary, patients with PDD or PD-MCI performed more poorly for most the cognitive tasks than patients with PD-CogNL or HCs did. PD-CogNL patients showed similar cognitive performance with HCs.

3.1. Region of interest for WM-related areas

The ROI masks for 16 WM-activated areas and 2 WM-deactivated areas are shown in Fig. 2. Coordinates for peak or center of mass and size of WM-related areas are described in Supplementary Table 1. Here, the right DLPFC mask consists of two separate brain-activated areas. They are described separately in Supplementary Table 1.

ROI masks for WM-activated areas included bilateral DLPFC, RPFC, frontal eye field (FEF), IPL/superior parietal lobule (SPL), anterior insular cortex (AIC), CdN/anterior lenticular nucleus (ALN), and middle temporal gyrus (MTG) and ACC and right precuneus (PCu). WM-deactivated areas included medial prefrontal cortex (MPFC) and PCC. (Fig. 2).

As a result, ROI masks for deactivated areas and the CdN were defined by $p < 2 \times 10^{-4}$ and voxel > 20. The cut-off was put on $p < 2 \times 10^{-9}$ and voxel > 20 in order to define separate ROI masks for WM-activated areas except the ROI mask for MTG which was defined by $p < 2 \times 10^{-5}$ and voxel > 20. BOLD effect estimates in each ROI for the two contrasts were quantified by using AFNI program: 3dROIstats. In the ROI analysis, the two separate right DLPFC areas were used as one right DLPFC ROI mask to estimate brain activation.

Table 1
Demographic and clinical data and n-back task performance.

	A	B	C	D		
Characteristics	HC (n = 17)	PD-CogNL (n = 18)	PD-MCI (n = 16)	PDD (n = 11)	*p*-value	Post-hoc significance
age	65.3 (6.5)	64.7 (5.1)	67.8 (5.1)	67.8 (7.6)	0.336	
sex [M/F]	13/4	12/6	11/5	11/0	0.190	
disease duration [years]	NA	7.8 (6.2)	8.2 (5.1)	10.1 (6.1)	0.573†	
education [years]	17.4 (2.0)	16.4 (1.9)	16.6 (2.1)	16.4 (2.7)	0.483	
MDS-UPDRS part I	NA	9.5 (5.2)	10.0 (4.7)	13.0 (5.7)	0.193†	
MDS-UPDRS part II	NA	10.4 (8.2)	8.4 (4.5)	15.5 (8.0)	0.042†	C < D*
MDS-UPDRS part III	NA	28.8 (20.1)	24.4 (12.5)	40.9 (8.3)	0.024†	C < D*
MDS-UPDRS part IV	NA	2.7 (2.7)	2.4 (2.4)	3.8 (3.3)	0.407†	
Hoehn–Yahr stage	NA	2.4 (0.5)	2.1 (0.5)	2.7 (0.8)	0.038†	C < D*
L-dopa equivalent dose	NA	836 (719)	617 (376)	734 (584)	0.555†	
MoCA score	28.2 (1.4)	28.3 (1.6)	24.7 (1.9)	21.5 (3.5)	<0.001	A > C,D***, B > C,D***, C > D*
n-back task performance						
0-back accuracy rate [%]	99.3 (1.5)	99.2 (1.4)	97.0 (3.9)	95.7 (5.0)	0.007	A,B > D*
1-back accuracy rate [%]	97.6 (3.9)	96.9 (3.6)	92.4 (8.7)	85.4 (10.7)	<0.001	A,B > D***
2-back accuracy rate [%]	96.3 (4.6)	94.1 (5.6)	88.4 (7.7)	73.5 (22.9)	<0.001	A,B > D***, C > D**
3-back accuracy rate [%]	86.3 (6.9)	84.5 (4.8)	80.0 (6.3)	68.6 (18.0)	<0.001	A,B > D***, C > D*
0-back d-prime index	4.0 (0.3)	4.0 (0.3)	3.6 (0.6)	3.4 (0.8)	0.017	B > D*
1-back d-prime index	3.8 (0.6)	3.6 (0.6)	3.1 (0.8)	2.3 (0.8)	<0.001	A,B > D***, C > D*
2-back d-prime index	3.6 (0.6)	3.1 (0.7)	2.4 (1.1)	1.5 (1.3)	<0.001	A,B > D***, A > C**
3-back d-prime index	2.1 (0.7)	1.8 (0.5)	1.3 (0.6)	0.9 (0.7)	<0.001	A > D***, B > D**
Number of BOLD components in ME-ICA analysis	18.1 (7.0)	17.8 (10.8)	19.1 (8.0)	19.4 (14.6)	0.97	

Data are presented as mean (standard deviation). HC = healthy control, PD = Parkinson's disease, PD-CogNL = cognitively normal PD, PD-MCI = PD with mild cognitive impairment, PDD = PD with dementia, MDS-UPDRS = Movement Disorder Society-Sponsored Revision of the Unified Parkinson's Disease Rating Scale, MoCA = Montreal - Cognitive Assessment, NA = not applicable, BOLD = Blood oxygenation level dependent, ME-ICA = multi-echo independent component analysis, † is inter-group comparison only in patient subgroups, *$P < 0.05$, **$P < 0.01$, *** $P < 0.01$ in post-hoc analysis.

Table 2
Neuropsychological properties.

	A	B	C	D		
Characteristics	HC (n = 17)	PD-CogNL (n = 18)	PD-MCI (n = 16)	PDD (n = 11)	p-value	Post-hoc significance
Neuropsychological tests						
BDI-II	2.2 (3.3)	9.8 (4.9)	8.1 (4.9)	7.9 (5.9)	<0.001	A < B***, A < C**, A < D*
MMSE score	29.5 (0.7)	29.4 (0.8)	28.6 (1.3)	26.8 (2.7)	<0.001	A,B > D***, C > D*
FAB score	17.8 (0.4)	17.4 (1.2)	16.3 (1.4)	14.1 (2.6)	0.001	A > C*, A,B > D***, C > D**
CVLT-II 1–5 (raw score)	59.4(9.1)	56.4(8.4)	50.3 (10.1)	42.5 (6.9)	<0.001	A > C*, A > D***, B > D**
memory subscores of MMSE	5.9 (0.2)	5.7 (0.5)	5.6 (0.5)	5.3 (0.8)	0.011	A > D**
Boston Naming test (T score)	50.9 (11.9)	55.8 (11.9)	51.3 (12.1)	43.7 (9.6)	0.072	B > D*
language subscores of MMSE	7.9 (0.2)	8.0 (0.0)	7.9 (0.2)	7.1 (1.4)	0.001	A,B,C > D**
Digit Span (scaled score)	12.9 (3.7)	12.7 (3.8)	10.1 (2.1)	9.4 (2.3)	0.005	A,B > D*
Letter Number Sequence (scaled score)	12.2 (2.7)	11.8 (2.5)	10.9 (1.6)	8.2 (2.1)	<0.001	A > D***, B > D**, C > D*
VOSP 1(raw score)	19.5 (1.0)	19.4 (1.2)	19.2 (1.0)	17.9 (1.4)	0.003	A,B > D**, C > D*
VOSP 2 (raw score)	20.2 (4.6)	21.4 (3.5)	19.8 (4.7)	16.7 (2.8)	0.032	B > D*
VOSP 3 (raw score)	17.5 (1.8)	17.5 (1.5)	17.2 (2.6)	14.6 (2.8)	0.004	A,B > D**, C > D*
VOSP 4 (raw score)	10.5 (3.8)	7.9 (2.4)	10.2 (2.3)	10.6 (3.1)	0.031	
VOSP 5 (raw score)	10.0 (0.0)	9.8 (0.4)	9.8 (0.4)	9.6 (0.7)	0.149	
VOSP 6 (raw score)	19.8 (1.0)	20.0 (0.0)	18.1 (4.8)	19.0 (1.5)	0.142	
VOSP 7 (raw score)	9.5 (1.2)	9.7 (0.6)	8.4 (1.8)	8.1 (2.0)	0.008	B > D*
VOSP 8 (raw score)	9.6 (1.2)	9.7 (0.5)	9.6 (0.6)	8.6 (1.2)	0.015	A,B > D*
WCST category	5.2 (1.6)	4.9 (1.9)	4.1 (2.1)	0.6 (0.7)	<0.001	A,B,C > D***
D-KEFS letter F (scaled score)	13.9 (3.7)	13.9 (3.8)	12.2 (3.4)	8.3 (3.6)	0.001	A,B > D**, C > D*
D-KEFS Category Fluency (scaled score)	13.4 (3.2)	13.9 (3.7)	12.0 (2.6)	7.5 (3.6)	<0.001	A,B > D***, C > D**
D-KEFS switch total (scaled score)	11.1 (3.4)	12.2 (3.6)	9.9 (2.8)	7.1 (3.4)	0.002	A > D*, B > D**
D-KEFS switch accuracy (scaled score)	10.6 (3.5)	11.0 (3.7)	10.4 (2.5)	6.8 (3.3)	0.01	A,C > D*, B > D**
D-KEFS Sorting test (scaled score)	13.2 (2.4)	13.8 (1.8)	11.1 (2.3)	7.8 (2.1)	<0.001	A > C*, A,B > D***, B > C**, C > D**
D-KEFS Sorting test description (scaled score)	12.7 (2.6)	12.9 (2.4)	10.3 (2.4)	6.4 (2.4)	<0.001	A > C*, A,B > D***, B > C**, C > D**
D-KEFS Tower (scaled score)	11.5 (3.6)	11.9 (3.4)	9.8 (2.2)	6.5 (3.0)	<0.001	A > D**, B > D***, C > D*
TMT-A (T score)	50.7 (11.8)	50.3 (11.3)	45.6 (8.9)	31.6 (11.2)	<0.001	A,B > D***, C > D**
TMT-B (T score)	51.4 (9.6)	51.8 (12.3)	46.9 (6.3)	32.4 (7.9)	<0.001	A,B > D***, C > D**
TMT-C (T score)	53.5 (8.0)	50.8 (11.3)	43.9 (9.9)	33.0 (12.6)	<0.001	A,B > D***

BDI-II = Beck Depression Inventory-II, MMSE = Mini-Mental State Examination, FAB = Frontal Assessment Battery, CVLT-II = The California Verbal Learning Test - II, VOSP = Visuospatial function: the Visual Object and Space Perception Battery, WCST = Wisconsin card sorting test, D-KEF = Delis-Kaplan Executive Function System, TMT = Trail making test, *$P < 0.05$, **$P < 0.01$, *** $P < 0.01$ in post-hoc analysis. See Fig. 1 legend for other abbreviations.

3.2. Inter-group comparisons of BOLD effect estimates vs. Fixation cross

In ROI analysis, BOLD effect estimates (vs. fixation cross) are shown in Fig. 3 and Supplementary Figs. 1 and 2. Bayesian multilevel model showed strong evidence in the following results. Here, "A had more activation than B" is expressed as A > B for simplicity. In summary, PD-CogNL > HCs or PD-MCI in most WM-activated areas in both the 2- and 3-back tasks. PD-CogNL > PDD in most WM-activated areas in the 3-

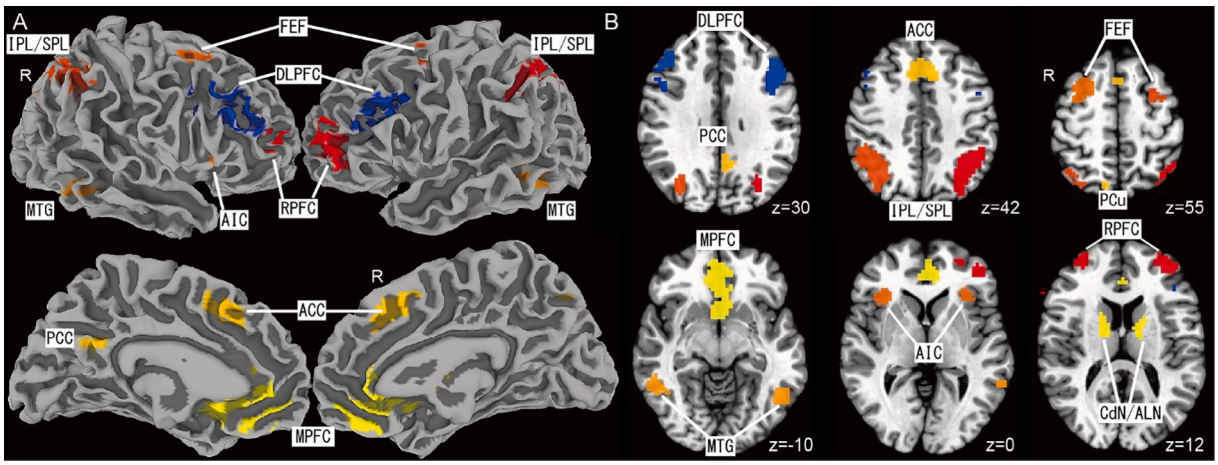

Fig. 2. Regions of interest (ROIs) for working memory-related areas. (A) lateral and medial view. (B) axial view. ACC = anterior cingulate cortex, AIC = anterior insular cortex, ALN = anterior lenticular nucleus, CdN = caudate nucleus, DLPFC = dorsolateral prefrontal cortex, FEF = frontal eye field, IPL = inferior parietal lobule, MFG = middle frontal gyrus, MTG = middle temporal gyrus, MPFC = medial prefrontal cortex, PCu = Precuneus, PCC = posterior cingulate cortex, RPFC = rostral prefrontal cortex, SPL = superior parietal lobule.

back task. PD-MCI > HCs in most WM-activated areas in both the 0- and 1-back tasks. PDD > HCs in all WM-activated areas in the 0- and 1-back tasks. PDD > PD-CogNL in most WM-activated areas in the 0-back task. In contrast, PCC was more deactivated in HCs or PD-CogNL patients than PDD patients in the 1-back task (Fig. 3).

3.3. Inter-group comparisons of BOLD effect estimates vs. 0-back task

In the ROI analysis, BOLD effect estimates (vs. 0-back task) are shown in Fig. 4 and Supplementary Figs. 3 and 4. In summary, HCs or PD-CogNL > PDD in most WM-activated areas in both the 2- and 3-back tasks. PD-CogNL > PDD in left FEF in the 1-back task. HCs > PDD in the left DLPFC and FEF in the 1-back task. On the other hand, MPFC and PCC were more deactivated in HCs than PD-CogNL in 2- and 3-back tasks (Fig. 4 and Supplementary Fig. 4).

3.4. Inter-task comparisons of BOLD effect estimates in each group

Inter-task comparisons between during 1-, 2- and 3-back task and during 0-back task are shown in Fig. 5. All WM-activated areas are more activated in HCs, PD-CogNL and PD-MCI (except left CdN/ALN in 3-back vs. 0-back). Only some WM-activated areas are more activated in PDD. PCC and MPFC are more deactivated in HCs and PD-MCI, but not PD-CogNL (except MPFC in 2-back vs. 0-back) or PDD. Inter-task comparisons between during 2- and 3-back task and during 1-back task are shown in Fig. 6. All WM-activated areas are more activated in HCs and PD-CogNL (except right mTL in 2- and 3-back vs. 1-back). Some (2-back) or limited (3-back) WM-activated areas are more activated in PD-MCI. No WM-activated areas are more activated in PDD. No areas are more activated during 3-back task than during 2-back task in all groups (Fig. 6).

3.5. Patterns of brain activations and deactivations for different loads

BOLD effect estimates were plotted for each n-back task in each group. Those for left DLPFC (Fig. 7A) and PCC (Fig. 7B) are shown. Based on inter-group comparisons (3.2 and 3.3 in Results) and inter-task comparisons (3.4), patterns of activation and deactivation are summarized as follows. HCs and PD-CogNL show a similar pattern of activation in most of WM-activated areas, including left DLPFC: 0-back < 1-back < 2- and 3-back. PDD shows a different pattern of activation: some of WM-activated areas, including left DLPFC, shows 0-back < 1-, 2- and 3-back, but other WM-activated areas are not different among 0-, 1-, 2-, and 3-back task. PD-MCI shows an intermediate pattern: left WM-activated areas, including left DLPFC, show a similar pattern with HCs and PD-CogNL, but other areas show a similar pattern with PDD. PDD have the highest activation during 0-back task. PD-CogNL have the highest activation during 2- and 3-back task. HCs tend to have the strongest deactivation at PCC during 3-back. PDD have less deactivation in PCC than other groups during 1-back and 3-back. d-prime index for each n-back task is shown in Fig. 7C.

3.6. Voxel-based correlation analysis for BOLD effect estimates and d-prime index

The voxel-based correlation analysis for all PD patients showed no significant correlation between BOLD effect estimates, when compared to the fixation cross, and the d-prime index. In contrast, BOLD effect estimates when compared to the 0-back task were correlated with the d-prime index in the following areas: bilateral DLPFC, left RPFC, left FEF/MFG, left AIC, left IPL/SPL, left CdN, right FEF/SFG and ACC for the 2-back task (Fig. 8A, see coordinates in Table 3), and left FEF/MFG, left PCu/IPL/SPL, right IPL/SPL, right PCu and right CdN/thalamus for the 3-back task (Fig. 8B, Table 3).

4. Discussion

This study evaluated the activation or deactivation in WM-related areas using ME-ICA analysis while performing the n-back task among PD patients with different levels of cognitive function. Our results showed that PD-CogNL patients have hyperactivation in WM-activated areas while performing moderate (2-back) and heavy WM (3-back) tasks, achieving normal WM. In contrast, PD-MCI and PDD patients have hyperactivation for the control (0-back) and light WM (1-back) tasks. Moreover, bilateral recruitment of WM-activated areas is associated with better performance in moderate and heavy WM load tasks in PD patients.

4.1. Altered brain activation patterns and neural correlates of WM deficit

We quantified BOLD effect estimates by comparing to either cross fixation or the 0-back task (Fig. 1A). The baseline in a general linear model when subjects were staring at a fixation cross was used as a task-free state. Performing 0-back task requires both cognitive and motor operations: i.e., paying attention to upcoming letters and pressing either the right or left button by responding to a prespecified letter or not,

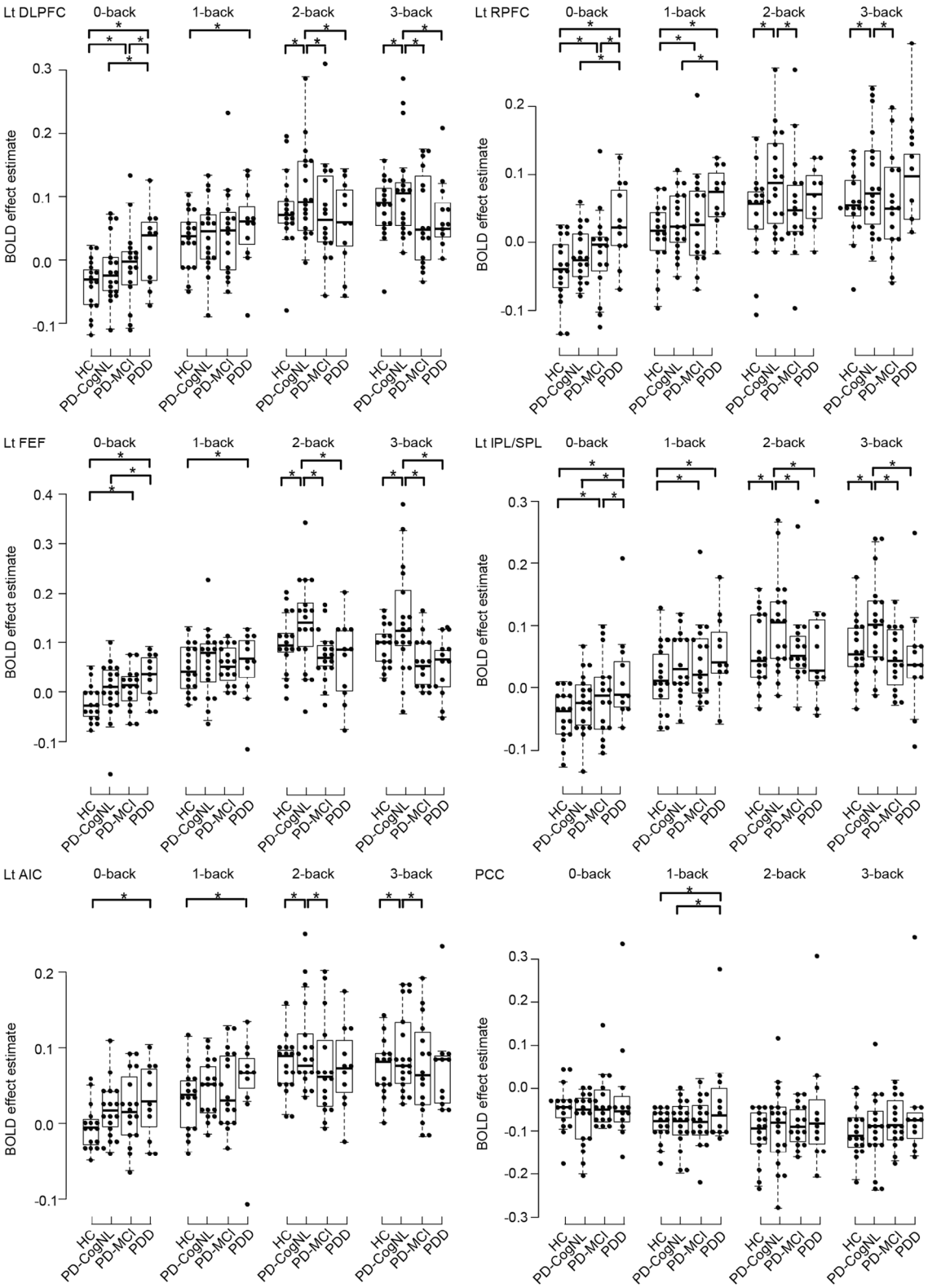

Fig. 3. Inter-group comparisons of BOLD effect estimate (vs. fixation cross). The results labeled with * are considered to have strong evidence for group difference in which the posterior probability of group difference being positive or negative is<0.05 under the Bayesian multilevel model. Lt = left. See other abbreviations in Figs. 1 and 2 legends.

respectively. Thus, two BOLD effect estimates (vs. fixation cross or vs. 0-back task) indicate different neural activity. BOLD effect estimates against fixation cross represent total activation from the baseline. On the other hand, BOLD effect estimates (vs. 0-back task) represent additional activation for WM on top of performing the control task (0-back task) (Fig. 1A). In the ROI analysis for BOLD effect estimates (vs. fixation cross) during 0-back task, patients with PD-MCI or PDD had more activation in most WM-activated areas than HCs. These results suggest that

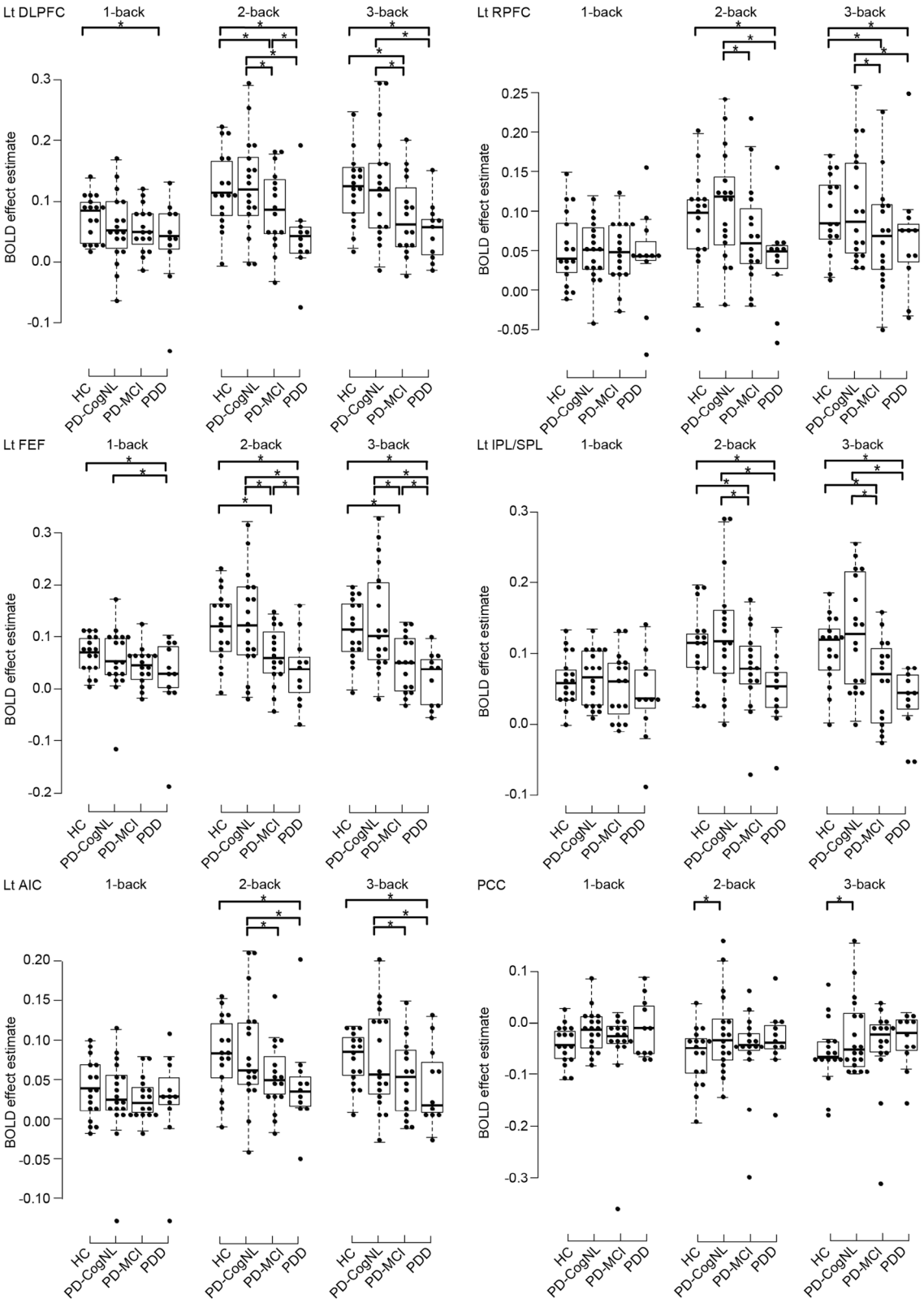

Fig. 4. Inter-group comparisons of BOLD effect estimate (vs. 0-back task). See explanation of * in Fig. 3 legend. See other abbreviations in Figs. 1, 2 and 3 legends.

the 0-back task is cognitively more demanding for PD-MCI or PDD patients than for HCs and requires more neural resources to perform. In other words, patients with PD-MCI or PDD have less neural resources to further activate for more demanding tasks (1-, 2-, 3-back task) on top of the control task (0-back). In the voxel-based correlation analysis, BOLD effect estimates (vs. fixation cross) are not correlated with the d-prime index in any n-back tasks. In contrast, when compared to 0-back task, BOLD effect estimates in specific WM-activated areas are correlated with the d-prime index in 2-back tasks (bilateral DLPFC, left RPFC, left FEF/MFG, left IPL, left SPL, left AIC, left CdN, right FEF/SFG, and ACC) and

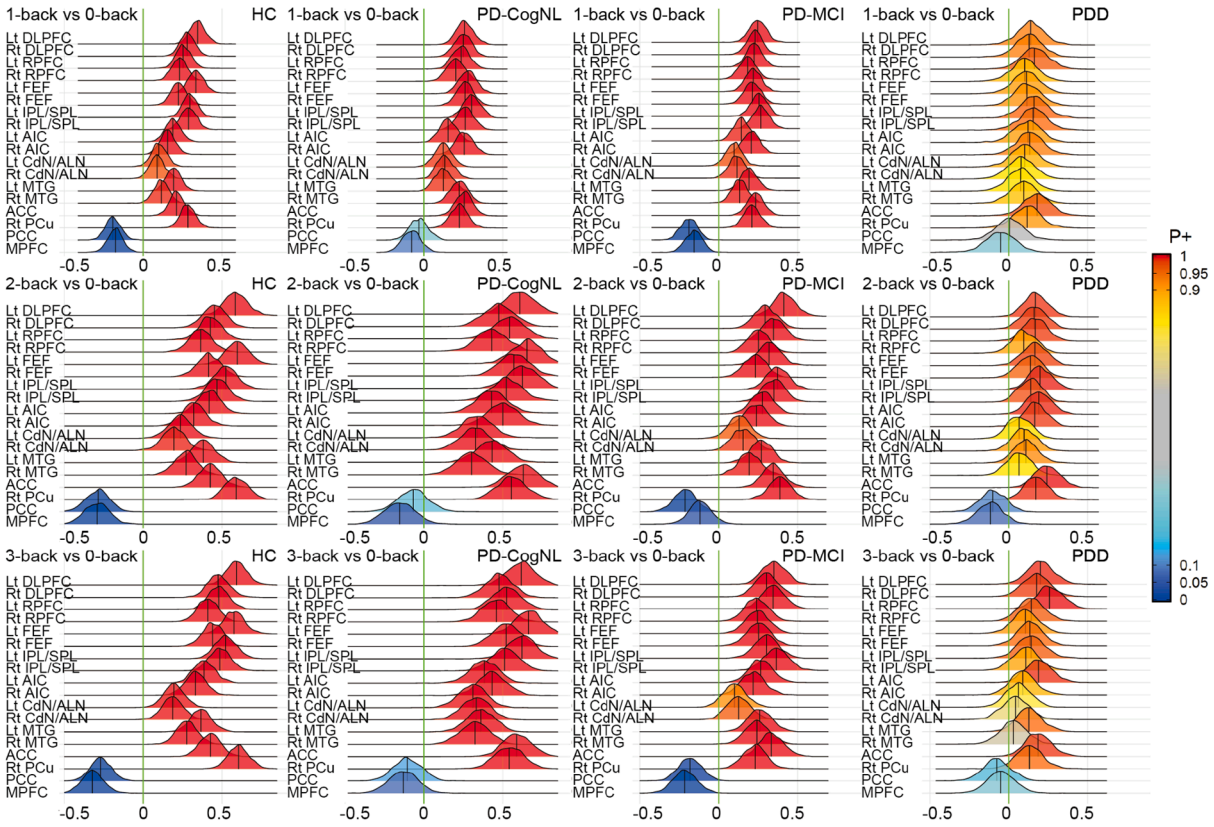

Fig. 5. Ridge plots for inter-task comparisons of BOLD effect estimate in each group. BOLD effect estimates in 1-, 2-, or 3-back were compared with those of 0-back. Each density shows the posterior distribution based on Bayesian multilevel modeling. Colors represent values of P+: the posterior probability of positive effect. The x-axis indicates effect magnitude in percent signal change. Rt = right. See abbreviations in Figs. 2 and 3 legends. More inter-task comparisons are showed in Fig. 6.

3-back task (left FEF/MFG, left PCu/IPL/SPL, right IPL/SPL, right CdN/thalamus and right PCu). Taken together, BOLD effect estimates (vs. 0-back task, not vs. fixation cross) are the neural correlates of WM in PD patients.

4.2. Roles of WM-activated areas

Multiple brain areas play different roles for performing WM. Here, BOLD effect estimates (vs. 0-back task) in bilateral DLPFC and left RPFC are related to 2-back task performance in PD patients. DLPFC plays an essential role in strategic control of WM, such as selecting appropriate high-level organizational chunks which reduces the overall cognitive load, enhancing task performance (Bor et al., 2004). RPFC may engage in parallel processing of multiple cognitive operations to achieve a goal (Ramnani and Owen, 2004). In fact, the N-back task is a typical task which requires complex and parallel processes. FEF is involved in eye movement as well as cognitive processes, reflecting the mental spotlight of attention (Thompson et al., 2005, Vernet et al., 2014). FEF and SPL form the dorsal attention network, which plays a role in goal-directed attentional orienting (Shomstein et al., 2010). In this study, BOLD effect estimates (vs. 0-back task) in left FEF are correlated with both 2- and 3-back task performances in PD patients, suggesting that left FEF is important for paying attention during a task. Right FEF is correlated with the 2-back task performance and may play a supplementary role to the left FEF. Left and right IPL store verbal WM (Jonides et al., 1998) and spatial WM (Smith and Jonides, 1998), respectively. Here, BOLD effect estimates (vs. 0-back task) in left IPL/SPL are correlated with the d-prime index in both 2- and 3-back tasks. However, the effect in right IPL/SPL is correlated with the d-prime index only in the 3-back task. Our results suggest that WM storage capacity in left IPL is critical for performance in 2-back and 3-back tasks. Right IPL may play a supplementary role for adding more storage capacity on top of left IPL, especially for 3-back task. Bilateral AIC and ACC form the salience network. This network is associated with detecting the stimuli which are salient to current goals (Seeley et al., 2007). ACC plays a role in detecting error (Carter et al., 1998). Here, left AIC and ACC are correlated with 2-back performance, possibly by keeping the subject alert for salient signal and detecting errors in WM processing. The CdN is a strategic region in which a single stroke causes dementia (Lanna et al., 2012). The CdN receives dense projections from the prefrontal cortex, forming a part of the striatothalamocortical loops (Shipp 2017). Moreover, the CdN is affected by dopaminergic denervation in PD patients. Here, activation in the left and right CdN is associated with performance in 2-back task and 3-back task, respectively. Thus, bilateral activation of the CdN may be a compensatory process to achieve better WM performance under the dopaminergic denervation in PD patients.

4.3. Compensatory mechanism for degenerating brain

Here, bilateral CdN/ALN (vs. fixation cross) were more activated in PD-CogNL patients than HCs during 2- and 3-back tasks, in PD-MCI patients than HCs during the 1-back task, and in PDD patients than HCs during 0- and 1-back tasks. Poston et al., (Poston et al., 2016) showed that PD-CogNL patients have hyperactivation of the bilateral putamen when off medication and dopaminergic medication downregulates this hyperactivation. Thus, dopaminergic medication status may modulate neural activations at least in some parts of brain in PD patients. In the current study, all PD patients took daily doses of anti-Parkinsonian medications as scheduled, and their medications might have partially normalized activation in CdN/ALN. A future study with dopaminergic medication ON/OFF is warranted to see how brain activations differ depending on medication status and cognitive status.

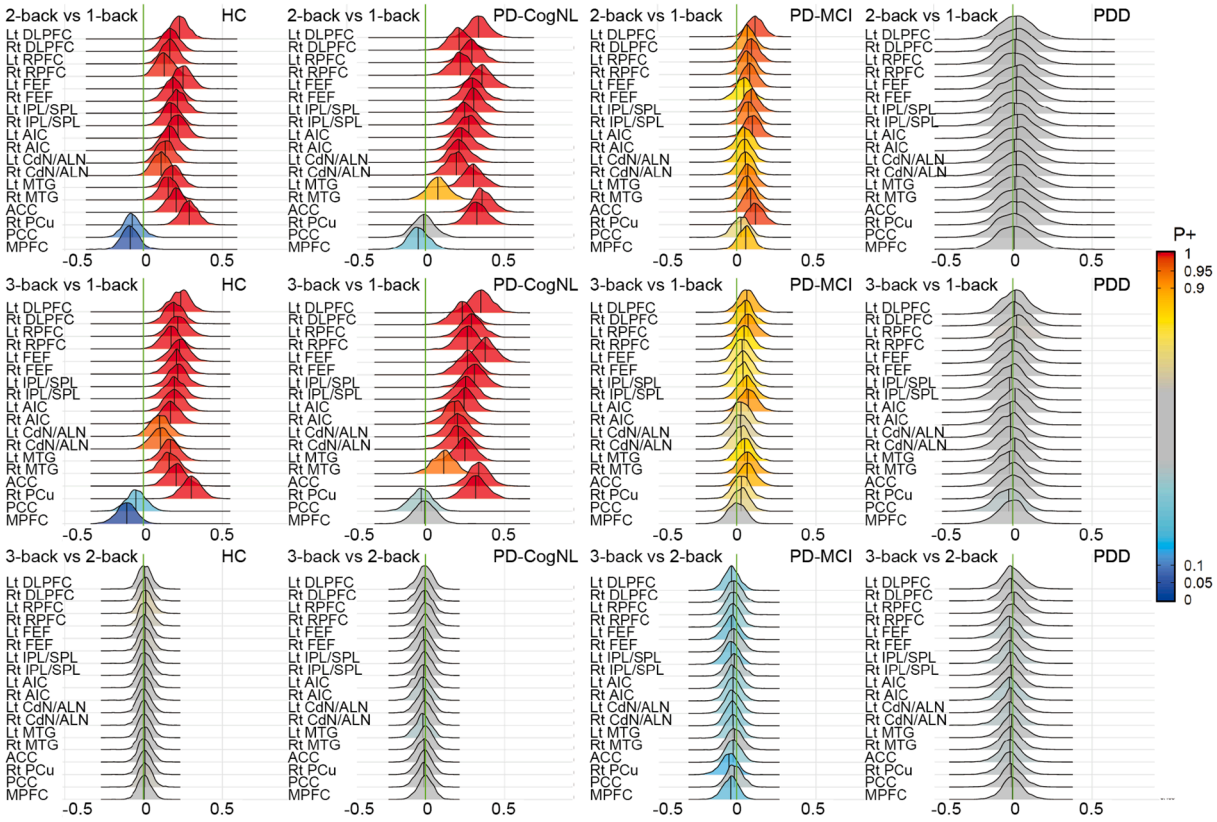

Fig. 6. (Continued from Fig. 5) Ridge plots for inter-task comparisons of BOLD effect estimate in each group. BOLD effect estimates in 2- or 3-back were compared with those of 1-back. BOLD effect estimates in 3-back were compared with those of 2-back. See Fig. 5 legend for explanations of density, color, and x-axis. See abbreviations in Figs. 2, 3 and 5 legends.

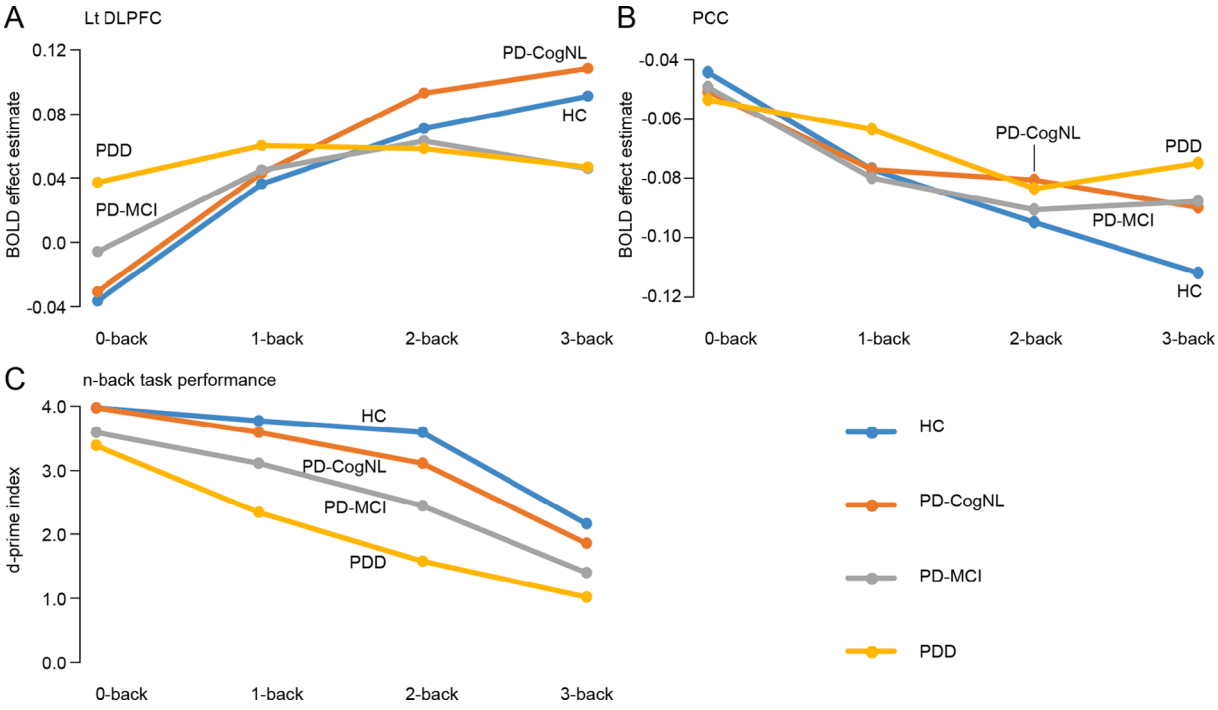

Fig. 7. Patterns of brain activations and deactivations and performances for different loads. Medians of BOLD effect estimates at left DLPFC (A) and PCC (B) during each n-back task are plotted in each group. N-back task performance is shown by using d-prime index (C). See abbreviations in Fig. 2 legend.

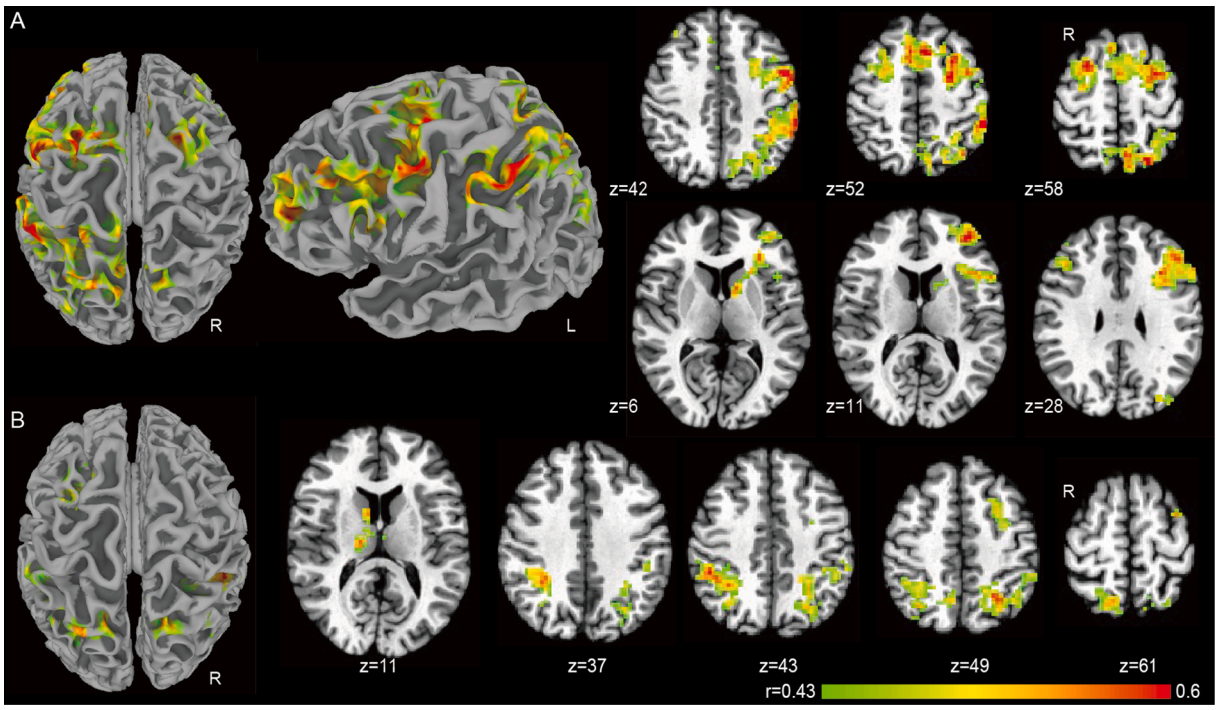

Fig. 8. The areas where BOLD effect estimates (vs. 0-back task) are significantly correlated with d-prime index in 2-back task (A) or in 3-back task (B). Correlation coefficients are shown by color, thresholded by r = 0.43.

Table 3
Coordinates where BOLD effect estimates (vs 0-back) are correlated with d-prime index.

			Coordinates						
			Center of Mass			Peak			
Region	side	Number of voxels	x	y	z	x	y	z	Correlation Coefficient
2-back task									
Left anterior complex		1771	−30	15	38				
DLPFC	L					−45	29	28	0.581
DLPFC	L					−49	4	42	0.661
RPFC	L					−39	48	11	0.622
FEF/MFG	L					−26	8	50	0.632
AIC	L					−30	31	6	0.570
ACC	M					−6	16	52	0.661
CdN	L					−12	7	4	0.571
DLPFC	R	114	40	37	28	42	25	28	0.535
Left posterior complex		993	−29	−55	52				
IPL	L					−53	−41	49	0.663
SPL	L					−24	−70	58	0.665
FEF/SFG	R	234	25	1	58	24	6.7	58	0.622
3-back task									
Left/Right posterior complex		474	−21	−59	48				
IPL/SPL	L					−27	−59	49	0.590
Pcu	R					12	−65	61	0.545
IPL/SPL	R	270	36	−49	44	48	−41	43	0.595
CdN/Thalamus	R	94	11	−8	14	9	5	11	0.548
FEF/MFG	L	83	−30	5	51	−36	1	61	0.539

L = left, R = right, M = middle, See legend of Fig. 1 for other abbreviations. Coordinates are reported in Montreal Neurological Institute (MNI) space.

Healthy elderly subjects hyperactivate the brain and recruit additional areas than young adults to perform less demanding tasks with similar performances to young adults, but underactivate the brain to perform more demanding tasks with impaired performances. This is known as the compensation-related utilization of neural circuits hypothesis (CRUNCH) (Reuter-Lorenz and Lustig, 2005, Reuter-Lorenz and Cappell, 2008). Here, PD patients have hyperactivation in WM-related areas for different WM loads depending on their cognitive status. Response curves for BOLD effect estimate and task demand are shown in Fig. 7. PD-CogNL patients have hyperactivation during 2- and 3-back tasks, maintaining normal WM performance (Table 1, Fig. 7C). On the other hand, PDD patients have hyperactivation during 0-back task with normal performance, but activation reaches almost plateau during 1-, 2- and 3-back tasks with impaired performance (Table 1, Fig. 7C). PD-MCI patients show intermediate pattern of PD-CogNL patients/HCs and PDD patients with impaired performance (Table 1, Fig. 7C). These patterns are similar to CRUNCH since hyperactivation is linked to maintaining normal WM performance.

Cabeza (2002) reported reduced functional hemispheric lateralization in the prefrontal cortex in healthy elderly adults compared to healthy young adults. This is called hemispheric asymmetry reduction in older adults (HAROLD). Here, bilateral recruitment of the brain is related to better WM performance; i.e., DLPFC and FEF for 2-back task and SPL/IPL for 3-back task. In addition, activations in the left CdN and right CdN are associated with better performance in 2-back and 3-back tasks, respectively. These patterns are similar to HAROLD since bilateral recruitments are related to better performance.

Cabeza et al. (2018) proposed two criteria to define compensation: First, it should be clear what is being compensated for. Second, it should be demonstrated that the enhanced activation is related to a beneficial effect on cognitive performance. For the first criterion, PD patients have deficits in multiple neurotransmitter systems such as dopamine (nigrostrial/mesocortical projections), acetylcholine, and norepinephrine (Gratwicke et al., 2015) as well as alpha-synuclein accumulation in diffuse brain areas, depending on the stage of disease (Braak et al., 2003). These neurodegenerations affect the WM-related areas as well (Gratwicke et al., 2015). Therefore, the hyperactivation likely compensates for the malfunctions of the degenerated brain regions in PD. In fact, the putamen has dopaminergic denervation in PD, and the hyperactivation in the putamen can be ameliorated by dopaminergic medication (Poston et al., 2016). For the second criterion, more activations and bilateral recruitment of certain areas, such as bilateral DLPFC, FEF, SPL/IPL, and CdN, are related to better WM performance in the correlation analysis (Fig. 8). Therefore, we interpret that PD patients use a CRUNCH/HAROLD-like compensatory mechanism to achieve better WM performance to deal with their degenerating brain.

Trujillo et al. (2015) demonstrated that de novo PD patients had hyperactivation in the bilateral DLPFC, left CdN, and left IPC while performing a visuospatial WM task compared to HCs. Furthermore, they also found that the DLPFC had reduced functional connectivity with other task-related regions in PD patients and altered effective connectivity within the frontoparietal network. They interpreted that the hyperactivation in WM-related areas is a compensatory mechanism to maintain behavioral performance in the presence of network deficits in PD patients. Here, PD patients had hyperactivation in WM-activated areas for different WM load tasks depending on their cognitive status. We speculate that PD patients have broad network deficits, including WM-activated areas, The different hyperactivation patterns at different stages of disease may be compensatory responses for progressing network abnormalities in PD patients. Future comparative analysis between activation and connectivity is warranted for PD patients with various cognitive deficits.

4.4. Altered deactivation pattern in default mode network

There are the anatomical areas that are deactivated while performing goal-directed activities such as the n-back task but are activated at rest. These areas are referred to as DMN (Shulman et al., 1997, Raichle et al., 2001, Raichle 2015). PCC and MPFC are two major nodes in DMN (Buckner et al., 2008). DMN exerts great influence on its anticorrelated networks, including WM-related areas (Uddin et al., 2009). Moreover, WM performance is associated with the functional interaction between the frontoparietal network; i.e., WM-related areas and DMN (Murphy et al., 2020). van Eimeren et al. (2009) reported that PD patients without dementia show comparable deactivation in MPFC, but less deactivation in PCC and the precuneus when performing executive tasks compared to HCs. However, no previous study explored patterns of deactivation in PCC or MPFC during n-back task among PD patients with different levels of cognitive function. Here, PDD patients have less deactivation in PCC than HCs or PD-CogNL patients during the 1-back task (Fig. 3). In addition, PD-CogNL patients have less deactivation (vs. 0-back task) in PCC and MPFC during 2- and 3-back tasks than HCs (Fig. 4 and Supplementary Fig. 4, respectively). Thus, PD-CogNL and PDD patients may have some functional abnormality in DMN. Hattori et al. (2012) showed that patients with PD-CogNL or PD-MCI have moderate hypoperfusion in PCC at rest, and PDD patients have remarkable hypoperfusion in PCC and moderate hypoperfusion in MPFC. However, both BOLD effect estimates (vs. fixation cross or 0-back task) in PCC and MPFC are not correlated with d-prime index in any n-back tasks in this study. Taken together, there is certain functional abnormality in DMN in PD patients that exacerbates over disease progression, but the extent of deactivation in DMN is not necessarily associated with WM performance.

4.5. Limitations

The study has several limitations. First, while it is known that WM function is affected by dopaminergic stimulation, all PD patients were evaluated on their daily anti-Parkinsonian medications to minimize motor symptoms and to let patients comfortably perform the n-back task. Although LED was not different among patient subgroups, different medications, in particular dopamine agonists, might modulate WM function differently. Evaluation for drug-naïve patients or during medication “OFF” state may be valuable to assess neural activation without or by minimizing therapeutic modification. Second, there are more male subjects in all groups. Thus, sex imbalance might affect our results. Third, we have limited sample size for each group. That might underestimate inter-group differences. Fourth, we used language and memory subscores of the MMSE to evaluate language and memory function. Since they are concise assessments, they might affect a patient’s classification. Fifth, we did not perform connectivity analysis during the n-back task. Activation and connectivity in WM-activated areas and WM-deactivated areas may play a supplementary role for each other, determining WM performance in PD patients. Future comparative studies of activation and connectivity are warranted. Sixth, while cognitive status was not used for ROI definition, a separate cohort would have been desirable. Seventh, we used fixation cross to quantify BOLD effect estimate during 0-, 1-, 2- and 3-back tasks. However, neural activities during fixation cross may be different among subjects and groups due to confounding effects of aging and neurodegeneration among others. On the other hand, differences of neural activity during the 0-back task among patients with different cognitive function has been typically neglected. Therefore, we aimed to explore BOLD effect estimate of 0-back task using fixation cross. fMRI can evaluate only relative extent of activation. This is limitation of all fMRI studies. In order to overcome this limitation, studies with other imaging modalities are warranted. Finally, since this is a cross-sectional study, we did not prove that PD patients actually develop the compensatory hyperactivation for different WM load tasks during disease progression. Future longitudinal studies are needed.

5. Conclusions

Our results suggest that additional activations in WM-activated areas on top of the 0-back task, rather than fixation cross, are neural correlates of WM performance in PD patients. Moreover, these patients have two types of compensatory mechanisms: (1) hyperactivation for different WM load tasks depending on their cognitive status, and (2) bilateral recruitment of WM-activated areas to improve WM performance.

6. Funding information

This research was supported by intramural funding by NIH and JSPS KAKENHI Grant Number 15K19803.

7. Ethics

This study was approved by Institutional Review Board of National Institute of Neurological Disorders and Stroke (NINDS), NIH. All the participants who had consent capacity gave their written informed consent to the study. For patients who did not have consent capacity, the

designated durable power of attorney delegate gave written informed consent.

CRediT authorship contribution statement

Takaaki Hattori: Conceptualization, Methodology, Investigation, Writing – original draft. **Richard Reynolds:** Methodology. **Edythe Wiggs:** Investigation. **Silvina G. Horovitz:** Methodology, Writing – review & editing. **Codrin Lungu:** Investigation. **Gang Chen:** Methodology, Software, Validation, Formal analysis, Writing – review & editing, Visualization. **Eiji Yasuda:** Software. **Mark Hallett:** Resources, Data curation, Writing – review & editing, Supervision, Project administration, Funding acquisition.

Declaration of Competing Interest

T.H. has received speaker's honoraria from Daiichi Sankyo Company, Limited; Sumitomo Dainippon Pharma Co., Ltd.; Integra Japan Co., Ltd and Kyowa Kirin Co., Ltd. R.R. has no disclosure. E.W. has no disclosure. S.H. has no disclosure. C.L. has honoraria for editorial work from Elsevier. G.C. has no disclosure. E.Y. has no disclosure. M.H. is an inventor of patents held by NIH for an immunotoxin for the treatment of focal movement disorders and the H-coil for magnetic stimulation; in relation to the latter, he has received license fee payments from the NIH (from Brainsway). He is on the Medical Advisory Boards of CALA Health and Brainsway (both unpaid positions). He is on the Editorial Board of approximately 15 journals and receives royalties and/or honoraria from publishing from Cambridge University Press, Oxford University Press, Springer, Wiley, Wolters Kluwer, and Elsevier. He has research grants from Medtronic, Inc. for a study of DBS for dystonia and CALA Health for studies of a device to suppress tremor.

Acknowledgements

We would like to thank Michael Tierney M.A. for performing some of the neuropsychological assessments; Elaine Considine, R.N. and Gayle McCrossin, R.N. for providing medical coverage during MRI scanning; and Devera G. Schoenberg, M.Sc., Editor, for editing the manuscript.

Appendix A. Supplementary data

Supplementary data to this article can be found online at https://doi.org/10.1016/j.nicl.2022.103100.

References

Aarsland, D., Zaccai, J., Brayne, C., 2005. A systematic review of prevalence studies of dementia in Parkinson's disease. Mov. Disord. 20 (10), 1255–1263. https://doi.org/10.1002/mds.20527.

Alexander, G.E., DeLong, M.R., Strick, P.L., 1986. Parallel organization of functionally segregated circuits linking basal ganglia and cortex. Annu. Rev. Neurosci. 9, 357–381. https://doi.org/10.1146/annurev.ne.09.030186.002041.

Antonelli, F., Strafella, A.P., 2014. Behavioral disorders in Parkinson's disease: the role of dopamine. Parkinsonism Relat. Disord. 20 (Suppl 1), S10–12. https://doi.org/10.1016/s1353-8020(13)70005-1.

Baddeley, A., 2010. Working memory. Curr. Biol. 20 (4), R136–140. https://doi.org/10.1016/j.cub.2009.12.014.

Baggio, H.C., Junqué, C., 2019. Functional MRI in Parkinson's Disease Cognitive Impairment. Int. Rev. Neurobiol. 144, 29–58. https://doi.org/10.1016/bs.irn.2018.09.010.

Beato, R., Levy, R., Pillon, B., Vidal, C., du Montcel, S.T., Deweer, B., Bonnet, A.M., Houeto, J.L., Dubois, B., Cardoso, F., 2008. Working memory in Parkinson's disease patients: clinical features and response to. Arq. Neuropsiquiatr. 66 (2a), 147–151.

Bor, D., Cumming, N., Scott, C.E., Owen, A.M., 2004. Prefrontal cortical involvement in verbal encoding strategies. Eur. J. Neurosci. 19 (12), 3365–3370. https://doi.org/10.1111/j.1460-9568.2004.03438.x.

Braak, H., Del Tredici, K., Rub, U., de Vos, R.A., Jansen Steur, E.N., Braak, E., 2003. Staging of brain pathology related to sporadic Parkinson's disease. Neurobiol. Aging 24 (2), 197–211 https://doi.org/S0197458002000659 [pii].

Buckner, R.L., Andrews-Hanna, J.R., Schacter, D.L., 2008. The brain's default network: anatomy, function, and relevance to disease. Ann. N. Y. Acad. Sci. 1124, 1–38. https://doi.org/10.1196/annals.1440.011.

Cabeza, R., 2002. Hemispheric asymmetry reduction in older adults: the HAROLD model. Psychol. Aging 17 (1), 85–100. https://doi.org/10.1037//0882-7974.17.1.85.

Cabeza, R., Albert, M., Belleville, S., Craik, F.I.M., Duarte, A., Grady, C.L., Lindenberger, U., Nyberg, L., Park, D.C., Reuter-Lorenz, P.A., Rugg, M.D., Steffener, J., Rajah, M.N., 2018. Maintenance, reserve and compensation: the cognitive neuroscience of healthy ageing. Nat. Rev. Neurosci. 19 (11), 701–710. https://doi.org/10.1038/s41583-018-0068-2.

Carter, C.S., Braver, T.S., Barch, D.M., Botvinick, M.M., Noll, D., Cohen, J.D., 1998. Anterior cingulate cortex, error detection, and the online monitoring of performance. Science 280 (5364), 747–749. https://doi.org/10.1126/science.280.5364.747.

Chen, G., Taylor, P. A., Stoddard, J., Cox, R. W., Bandettini, P. A. and Pessoa, L., 2021. Sources of information waste in neuroimaging: mishandling structures, thinking dichotomously, and over-reducing data. bioRxiv 2021.2005.2009.443246. doi: 10.1101/2021.05.09.443246.

Chen, G., Xiao, Y., Taylor, P.A., Rajendra, J.K., Riggins, T., Geng, F., Redcay, E., Cox, R. W., 2019. Handling multiplicity in neuroimaging through Bayesian lenses with multilevel modeling. Neuroinformatics 17 (4), 515–545. https://doi.org/10.1007/s12021-018-9409-6.

Chen, G., Taylor, P.A., Cox, R.W., Pessoa, L., 2020. Fighting or embracing multiplicity in neuroimaging? Neighborhood leverage versus global calibration. Neuroimage 206, 116320. https://doi.org/10.1016/j.neuroimage.2019.116320.

Cox, R.W., 1996. AFNI: software for analysis and visualization of functional magnetic resonance neuroimages. Comput. Biomed. Res. 29 (3), 162–173. https://doi.org/10.1006/cbmr.1996.0014.

Dirnberger, G., Jahanshahi, M., 2013. Executive dysfunction in Parkinson's disease: a review. J. Neuropsychol. 7 (2), 193–224. https://doi.org/10.1111/jnp.12028.

Dubois, B., Burn, D., Goetz, C., Aarsland, D., Brown, R.G., Broe, G.A., Dickson, D., Duyckaerts, C., Cummings, J., Gauthier, S., Korczyn, A., Lees, A., Levy, R., Litvan, I., Mizuno, Y., McKeith, I.G., Olanow, C.W., Poewe, W., Sampaio, C., Tolosa, E., Emre, M., 2007. Diagnostic procedures for Parkinson's disease dementia: recommendations from the movement disorder society task force. Mov. Disord. 22 (16), 2314–2324. https://doi.org/10.1002/mds.21844.

Ekman, U., Eriksson, J., Forsgren, L., Mo, S.J., Riklund, K., Nyberg, L., 2012. Functional brain activity and presynaptic dopamine uptake in patients with Parkinson's disease and mild cognitive impairment: a cross-sectional study. Lancet Neurol. 11 (8), 679–687. https://doi.org/10.1016/s1474-4422(12)70138-2.

Emre, M., Aarsland, D., Brown, R., Burn, D.J., Duyckaerts, C., Mizuno, Y., Broe, G.A., Cummings, J., Dickson, D.W., Gauthier, S., Goldman, J., Goetz, C., Korczyn, A., Lees, A., Levy, R., Litvan, I., McKeith, I., Olanow, W., Poewe, W., Quinn, N., Sampaio, C., Tolosa, E., Dubois, B., 2007. Clinical diagnostic criteria for dementia associated with Parkinson's disease. Mov. Disord. 22 (12), 1689–1707. https://doi.org/10.1002/mds.21507 quiz 1837.

Giehl, K., Tahmasian, M., Eickhoff, S.B., van Eimeren, T., 2019. Imaging executive functions in Parkinson's disease: An activation likelihood estimation meta-analysis. Parkinsonism Relat. Disord. 63, 137–142. https://doi.org/10.1016/j.parkreldis.2019.02.015.

Goetz, C.G., Tilley, B.C., Shaftman, S.R., Stebbins, G.T., Fahn, S., Martinez-Martin, P., Poewe, W., Sampaio, C., Stern, M.B., Dodel, R., Dubois, B., Holloway, R., Jankovic, J., Kulisevsky, J., Lang, A.E., Lees, A., Leurgans, S., LeWitt, P.A., Nyenhuis, D., Olanow, C.W., Rascol, O., Schrag, A., Teresi, J.A., van Hilten, J.J., LaPelle, N., 2008. Movement Disorder Society-sponsored revision of the Unified Parkinson's Disease Rating Scale (MDS-UPDRS): scale presentation and clinimetric testing results. Mov. Disord. 23 (15), 2129–2170. https://doi.org/10.1002/mds.22340.

Goldman, J.G., Williams-Gray, C., Barker, R.A., Duda, J.E., Galvin, J.E., 2014. The spectrum of cognitive impairment in Lewy body diseases. Mov. Disord. 29 (5), 608–621. https://doi.org/10.1002/mds.25866.

Gonzalez-Castillo, J., Panwar, P., Buchanan, L.C., Caballero-Gaudes, C., Handwerker, D. A., Jangraw, D.C., Zachariou, V., Inati, S., Roopchansingh, V., Derbyshire, J.A., Bandettini, P.A., 2016. Evaluation of multi-echo ICA denoising for task based fMRI studies: Block designs, rapid event-related designs, and cardiac-gated fMRI. Neuroimage 141, 452–468. https://doi.org/10.1016/j.neuroimage.2016.07.049.

Gratwicke, J., Jahanshahi, M., Foltynie, T., 2015. Parkinson's disease dementia: a neural networks perspective. Brain 138 (Pt 6), 1454–1476. https://doi.org/10.1093/brain/awv104.

Haatveit, B.C., Sundet, K., Hugdahl, K., Ueland, T., Melle, I., Andreassen, O.A., 2010. The validity of d prime as a working memory index: results from the "Bergen n-back task". J. Clin. Exp. Neuropsychol. 32 (8), 871–880. https://doi.org/10.1080/13803391003596421.

Hattori, T., Orimo, S., Aoki, S., Ito, K., Abe, O., Amano, A., Sato, R., Sakai, K., Mizusawa, H., 2012. Cognitive status correlates with white matter alteration in Parkinson's disease. Hum. Brain Mapp. 33 (3), 727–739. https://doi.org/10.1002/hbm.21245.

Hughes, A.J., Daniel, S.E., Kilford, L., Lees, A.J., 1992. Accuracy of clinical diagnosis of idiopathic Parkinson's disease: a clinico-pathological study of 100 cases. J. Neurol. Neurosurg. Psychiatry 55 (3), 181–184. https://doi.org/10.1136/jnnp.55.3.181.

Jonides, J., Schumacher, E.H., Smith, E.E., Koeppe, R.A., Awh, E., Reuter-Lorenz, P.A., Marshuetz, C., Willis, C.R., 1998. The role of parietal cortex in verbal working memory. J. Neurosci. 18 (13), 5026–5034. https://doi.org/10.1523/jneurosci.18-13-05026.1998.

Kirchner, W.K., 1958. Age differences in short-term retention of rapidly changing information. J. Exp. Psychol. 55 (4), 352–358. https://doi.org/10.1037/h0043688.

Klein, M.O., Battagello, D.S., Cardoso, A.R., Hauser, D.N., Bittencourt, J.C., Correa, R.G., 2019. Dopamine: functions, signaling, and association with neurological diseases. Cell. Mol. Neurobiol. 39 (1), 31–59. https://doi.org/10.1007/s10571-018-0632-3.

Kundu, P., Inati, S.J., Evans, J.W., Luh, W.M., Bandettini, P.A., 2012. Differentiating BOLD and non-BOLD signals in fMRI time series using multi-echo EPI. Neuroimage 60 (3), 1759–1770. https://doi.org/10.1016/j.neuroimage.2011.12.028.

Kundu, P., Voon, V., Balchandani, P., Lombardo, M.V., Poser, B.A., Bandettini, P.A., 2017. Multi-echo fMRI: a review of applications in fMRI denoising and analysis of BOLD signals. Neuroimage 154, 59–80. https://doi.org/10.1016/j.neuroimage.2017.03.033.

Lanna, M.E., Alves, C.E., Sudo, F.K., Alves, G., Valente, L., Moreira, D.M., Cavalcanti, J. L., Engelhardt, E., 2012. Cognitive disconnective syndrome by single strategic strokes in vascular dementia. J. Neurol. Sci. 322 (1–2), 176–183. https://doi.org/10.1016/j.jns.2012.08.004.

Lewis, S.J., Cools, R., Robbins, T.W., Dove, A., Barker, R.A., Owen, A.M., 2003a. Using executive heterogeneity to explore the nature of working memory deficits in Parkinson's disease. Neuropsychologia 41 (6), 645–654. https://doi.org/10.1016/s0028-3932(02)00257-9.

Lewis, S.J., Dove, A., Robbins, T.W., Barker, R.A., Owen, A.M., 2003b. Cognitive impairments in early Parkinson's disease are accompanied by reductions in activity in frontostriatal neural circuitry. J. Neurosci. 23 (15), 6351–6356. https://doi.org/10.1523/jneurosci.23-15-06351.2003.

Lewis, S.J., Slabosz, A., Robbins, T.W., Barker, R.A., Owen, A.M., 2005. Dopaminergic basis for deficits in working memory but not attentional set-shifting in Parkinson's disease. Neuropsychologia 43 (6), 823–832. https://doi.org/10.1016/j.neuropsychologia.2004.10.001.

Litvan, I., Goldman, J.G., Troster, A.I., Schmand, B.A., Weintraub, D., Petersen, R.C., Mollenhauer, B., Adler, C.H., Marder, K., Williams-Gray, C.H., Aarsland, D., Kulisevsky, J., Rodriguez-Oroz, M.C., Burn, D.J., Barker, R.A., Emre, M., 2012. Diagnostic criteria for mild cognitive impairment in Parkinson's disease: Movement Disorder Society Task Force guidelines. Mov. Disord. 27 (3), 349–356. https://doi.org/10.1002/mds.24893.

Macdonald, P.A., Monchi, O., 2011. Differential effects of dopaminergic therapies on dorsal and ventral striatum in Parkinson's disease: implications for cognitive function. Parkinsons Dis. 2011, 572743 https://doi.org/10.4061/2011/572743.

Murphy, A.C., Bertolero, M.A., Papadopoulos, L., Lydon-Staley, D.M., Bassett, D.S., 2020. Multimodal network dynamics underpinning working memory. Nat. Commun. 11 (1), 3035. https://doi.org/10.1038/s41467-020-15541-0.

Muslimovic, D., Post, B., Speelman, J.D., Schmand, B., 2005. Cognitive profile of patients with newly diagnosed Parkinson disease. Neurology 65 (8), 1239–1245. https://doi.org/10.1212/01.wnl.0000180516.69442.95.

Oades, R.D., Halliday, G.M., 1987. Ventral tegmental (A10) system: neurobiology. 1. Anatomy and connectivity. Brain Res. 434 (2), 117–165. https://doi.org/10.1016/0165-0173(87)90011-7.

Ogawa, S., Lee, T.M., Kay, A.R., Tank, D.W., 1990. Brain magnetic resonance imaging with contrast dependent on blood oxygenation. Proc. Natl. Acad. Sci. U.S.A. 87 (24), 9868–9872. https://doi.org/10.1073/pnas.87.24.9868.

Owen, A.M., McMillan, K.M., Laird, A.R., Bullmore, E., 2005. N-back working memory paradigm: a meta-analysis of normative functional neuroimaging studies. Hum. Brain Mapp. 25 (1), 46–59. https://doi.org/10.1002/hbm.20131.

Poewe, W., Seppi, K., Tanner, C.M., Halliday, G.M., Brundin, P., Volkmann, J., Schrag, A. E., Lang, A.E., 2017. Parkinson disease. Nat. Rev. Dis. Primers 3, 17013. https://doi.org/10.1038/nrdp.2017.13.

Poston, K.L., YorkWilliams, S., Zhang, K., Cai, W., Everling, D., Tayim, F.M., Llanes, S., Menon, V., 2016. Compensatory neural mechanisms in cognitively unimpaired Parkinson disease. Ann. Neurol. 79 (3), 448–463. https://doi.org/10.1002/ana.24585.

Raichle, M.E., 2015. The brain's default mode network. Annu. Rev. Neurosci. 38, 433–447. https://doi.org/10.1146/annurev-neuro-071013-014030.

Raichle, M.E., MacLeod, A.M., Snyder, A.Z., Powers, W.J., Gusnard, D.A., Shulman, G.L., 2001. A default mode of brain function. Proc. Natl. Acad. Sci. U.S.A. 98, 676–682.

Ramnani, N., Owen, A.M., 2004. Anterior prefrontal cortex: insights into function from anatomy and neuroimaging. Nat. Rev. Neurosci. 5 (3), 184–194. https://doi.org/10.1038/nrn1343.

Reuter-Lorenz, P., Cappell, K., 2008. Neurocognitive aging and the compensation hypothesis. Curr. Directions Psychol. Sci. 17, 177–182. https://doi.org/10.1111/j.1467-8721.2008.00570.x.

Reuter-Lorenz, P.A., Lustig, C., 2005. Brain aging: reorganizing discoveries about the aging mind. Curr. Opin. Neurobiol. 15 (2), 245–251. https://doi.org/10.1016/j.conb.2005.03.016.

Seeley, W.W., Menon, V., Schatzberg, A.F., Keller, J., Glover, G.H., Kenna, H., Reiss, A.L., Greicius, M.D., 2007. Dissociable intrinsic connectivity networks for salience processing and executive control. J. Neurosci. United States. 27, 2349–2356.

Shipp, S., 2017. The functional logic of corticostriatal connections. Brain Struct. Funct. 222 (2), 669–706. https://doi.org/10.1007/s00429-016-1250-9.

Shomstein, S., Lee, J., Behrmann, M., 2010. Top-down and bottom-up attentional guidance: investigating the role of the dorsal and ventral parietal cortices. Exp. Brain Res. 206 (2), 197–208. https://doi.org/10.1007/s00221-010-2326-z.

Shulman, G.L., Fiez, J.A., Corbetta, M., Buckner, R.L., Miezin, F.M., Raichle, M.E., Petersen, S.E., 1997. Common blood flow changes across visual tasks: II. Decreases in cerebral cortex. J. Cogn. Neurosci. 9 (5), 648–663. https://doi.org/10.1162/jocn.1997.9.5.648.

Smith, E.E., Jonides, J., 1998. Neuroimaging analyses of human working memory. Proc. Natl. Acad. Sci. U.S.A. 95 (20), 12061–12068. https://doi.org/10.1073/pnas.95.20.12061.

Svenningsson, P., Westman, E., Ballard, C., Aarsland, D., 2012. Cognitive impairment in patients with Parkinson's disease: diagnosis, biomarkers, and treatment. Lancet Neurol. 11 (8), 697–707. https://doi.org/10.1016/s1474-4422(12)70152-7.

Thompson, K.G., Biscoe, K.L., Sato, T.R., 2005. Neuronal basis of covert spatial attention in the frontal eye field. J. Neurosci. 25 (41), 9479–9487. https://doi.org/10.1523/jneurosci.0741-05.2005.

Tomlinson, C.L., Stowe, R., Patel, S., Rick, C., Gray, R., Clarke, C.E., 2010. Systematic review of levodopa dose equivalency reporting in Parkinson's disease. Mov. Disord. 25 (15), 2649–2653. https://doi.org/10.1002/mds.23429.

Trujillo, J.P., Gerrits, N.J., Veltman, D.J., Berendse, H.W., van der Werf, Y.D., van den Heuvel, O.A., 2015. Reduced neural connectivity but increased task-related activity during working memory in de novo Parkinson patients. Hum. Brain Mapp. 36 (4), 1554–1566. https://doi.org/10.1002/hbm.22723.

Uddin, L.Q., Kelly, A.M., Biswal, B.B., Castellanos, F.X., Milham, M.P., 2009. Functional connectivity of default mode network components: correlation, anticorrelation, and causality. Hum. Brain Mapp. 30 (2), 625–637. https://doi.org/10.1002/hbm.20531.

van Eimeren, T., Monchi, O., Ballanger, B., Strafella, A.P., 2009. Dysfunction of the default mode network in Parkinson disease: a functional magnetic resonance imaging study. Arch. Neurol. United States. 66, 877–883.

Vernet, M., Quentin, R., Chanes, L., Mitsumasu, A., Valero-Cabre, A., 2014. Frontal eye field, where art thou? Anatomy, function, and non-invasive manipulation of frontal regions involved in eye movements and associated cognitive operations. Front. Integr. Neurosci. 8, 66. https://doi.org/10.3389/fnint.2014.00066.

Wang, Y.P., Gorenstein, C., 2013. Psychometric properties of the Beck Depression Inventory-II: a comprehensive review. Braz. J. Psychiatry 35 (4), 416–431. https://doi.org/10.1590/1516-4446-2012-1048.

Weintraub, D., Simuni, T., Caspell-Garcia, C., Coffey, C., Lasch, S., Siderowf, A., Aarsland, D., Barone, P., Burn, D., Chahine, L.M., Eberling, J., Espay, A.J., Foster, E. D., Leverenz, J.B., Litvan, I., Richard, I., Troyer, M.D., Hawkins, K.A., 2015. Cognitive performance and neuropsychiatric symptoms in early, untreated Parkinson's disease. Mov. Disord. 30 (7), 919–927. https://doi.org/10.1002/mds.26170.